

Synthesis and Characterization of Copper Oxide Nanoparticles Using Polyol and Their Antimicrobial Potential

Rashmi Khulbe ^{1,*} , Rajesh Kumar ¹, Vinod Kumar ², Asha Kandpal ¹, Rajendra Joshi ¹, Bhuwan Chandra ¹, N.D. Kandpal ¹

¹ Department of Chemistry, Kumaun University, S.S.J. Campus, Almora-263601, Uttarakhand, India

² Department of Chemistry, School of Sciences, Uttarakhand Open University, Haldwani (Nainital)-263139, Uttarakhand, India

* Correspondence: rashmikhulbe00@gmail.com (R.K.);

Scopus Author ID 58222613400

Received: 3.05.2023; Accepted: 28.05.2023; Published: 19.02.2024

Abstract: In the present study, the copper oxide nanoparticles were synthesized via a green approach in polyol and cow milk using copper acetate salt as a precursor. The synthesized copper oxide nanoparticles were characterized using X-ray diffraction (XRD), Fourier transform infrared spectroscopy (FTIR), ultraviolet-visible spectroscopy, transmission electron microscopy (TEM), and scanning electron microscopy-energy dispersive X-ray (SEM-EDX) techniques. By employing the Debye-Scherrer equation, the X-ray diffraction (XRD) findings reveal that the average crystallite size of the synthesized nanoparticles is approximately 21 nm. As per the TEM report, the particle sizes of synthesized nanoparticles were found to be 23 nm. Synthesized copper oxide nanoparticles were analyzed against various bacterial strains (*Bacillus subtilis*, *B. megaterium*, *Escherichia coli*, and *Serratia marcescens*) and fungal pathogens (*Fusarium solani*, *Paecilomyces variotii*, *Trametes hirsuta*, and *Pythium afertile*). Among these microbes, copper oxide nanoparticles showed antibacterial activity against only *E. coli* (16 ± 0.6 mm) and inhibition potential against fungal pathogens *Trametes hirsuta* and *Fusarium solani*

Keywords: antimicrobial potential; copper oxide nanoparticles; green synthesis; milk; polyol method.

© 2024 by the authors. This article is an open-access article distributed under the terms and conditions of the Creative Commons Attribution (CC BY) license (<https://creativecommons.org/licenses/by/4.0/>).

1. Introduction

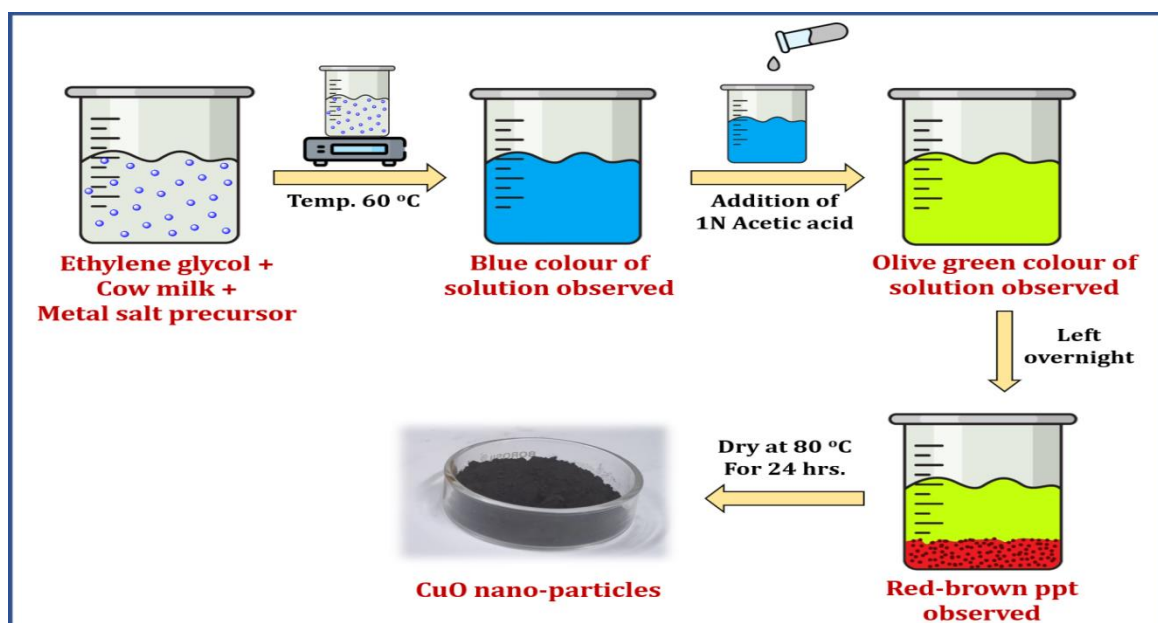
Copper oxide nanoparticles have special importance in the research area of nanotechnology; numerous studies are on the subject [1-4]. These studies deal with various aspects such as size, morphology, crystallinity, and synthesis of nanoparticles, which leads to improving their specific characteristics. Precursors [5], method of preparation [6, 7], temperature [8, 9], and other physicochemical conditions [10, 11] affect the synthesis of copper oxide nanoparticles. Copper oxide nanoparticles can be synthesized by various methods such as the microwave-assisted method [12], sol-gel method [13], hydrothermal process [14], and chemical deposition method [15]. Solution-based processing routes used in the synthesis of nanoparticles include precipitation of solids from supersaturated solutions, liquid phase, chemical reduction, and decomposition of chemical precursors with ultrasonic waves. CuO nanoparticle exhibits excellent antimicrobial activity. It has been reported earlier that a suitable dose of copper oxide nanoparticles can kill gram-positive and gram-negative bacteria within 2

hours of exposure; smaller size and higher positive surface charge enhance the toxicity of nanoparticles [16]. CuO is a p-type metal oxide semiconductor with distinctive electrical, optical, and catalytic properties. [17].

A report on the synthesis of copper oxide nanoparticles through a wet process produced in the form of Cu₂O in an acid medium and CuO in a basic medium from copper acetate [18, 19]. This study drew our attention to altering the formation of specific oxide in an acidic medium by changing the composition of reagents or by adding other products, especially biomaterials such as starch, milk, *Sapindus mukorossi* plant extract, etc. Though nanoparticles of copper oxide have been synthesized by the polyol method without taking acid/base, in these syntheses, the copper ion forms a solvation sphere with polyol and water, which results in the reduction of copper salts into its oxides and copper metal. Still, there are few reports available on the synthesis of nanoparticles using cow milk with metal salts [20-22]. In this study, we were interested in examining the possibility of the green synthesis route using cow milk. Proteins and sugars are constituents of milk that have reducing properties towards metal ions. Moreover, the operating temperature of our synthesis does not compromise the functional properties of milk. In the present study, it has been confirmed for the first time that copper oxide nanoparticles can be synthesized using cow milk by adjusting the concentration of acid and ethylene glycol. Acetic acid used in the synthesis belongs to the class of less toxic chemicals, which supports the safe approach for synthesizing copper oxide nanoparticles. This primary investigation can also give a clear picture of the new polyol synthesis, which is unavailable yet.

2. Materials and Methods

Copper (II) Acetate monohydrate (Cu(CH₃COO)₂.H₂O) was purchased from Molychem, India, as a precursor for copper oxide nanoparticles and ethylene glycol. Cow milk was obtained from a local market (Almora, Uttarakhand, India). All chemicals were used as received without any treatment. Double distilled water (conductivity < 1.0 μS_{cm}⁻¹ at room temperature) was used throughout the experiment.



Scheme 1. Schematic diagram for the synthesis of Copper oxide nanoparticles

The synthesis of copper oxide nanoparticles was carried out using biomaterial (milk) in order to establish the method of preparation of metal nanoparticles through the green route (Scheme 1). To synthesize copper oxide nanoparticles, copper acetate monohydrate was dissolved in 9:1 ethylene glycol and milk mixture to get 0.1 M copper acetate solution. The reaction solution was kept on the hot plate, continuously and steadily stirred for 1 hour at 60°C, and then allowed to cool at room temperature. After cooling, 1 N acetic acid solution (~20 mL of acetic acid) was added drop by drop (pH~4.06), and the color of the solution became olive green from blue. The solution was heated for half an hour at 60°C with continuous stirring. The dark brown-red precipitate obtained from the solution indicated the formation of copper oxide nanoparticles. The precipitate formed was collected by centrifugation, washed three times with ethanol and distilled water, and dried at room temperature. The dried sample was kept in the oven for 24 hours at a temperature of 80°C. The sample was ground with hand mortar to get the fine powdered form of nanoparticles. The sample was heated at 200°C before characterization.

3. Results and Discussion

3.1. Characterization of CuO nanoparticles.

Phase purity and crystallite size of synthesized copper oxide nanoparticles were characterized by Philips X'pert MPD System with copper K α radiation ($\lambda=0.154$ nm and 2θ ranging from 5.0129 to 79.9709°).

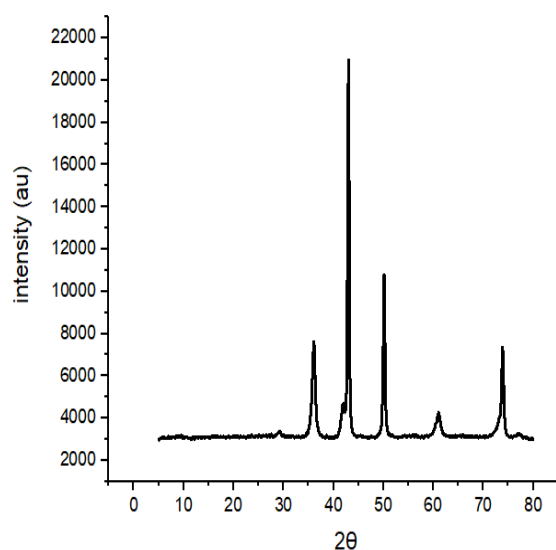


Figure 1. X-ray diffraction pattern of synthesized copper oxide nanoparticles.

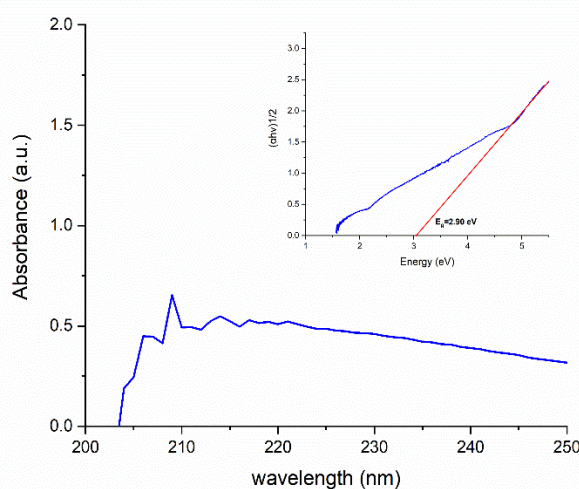


Figure 2. UV-Vis spectra of synthesized copper oxide nanoparticles.

The XRD pattern of synthesized nanoparticles is shown in Figure 1, revealing that synthesized copper oxide nanoparticles are crystalline and pure. All XRD peaks are observed at 2θ values of 35-74° which correspond to the planes indexed at (110), (111), (202), (113), and (311) and indicate the synthesis of CuO in monoclinic crystal phase [23]. These results are comparable with previously reported data [24, 25]. The crystallite size of synthesized nanoparticles was calculated with the help of the Debye-Scherrer equation [26].

$$D = \frac{k\lambda}{\beta \cos\theta} \dots \dots \dots (1)$$

where, k is a constant ($=0.9$), λ is the wavelength of X-rays ($=0.154$ nm), β is the full width half maximum length, and θ is the half diffraction angle. The crystallite size of synthesized nanoparticles ranges from 13 nm to 28 nm, and the average crystallite size is estimated to be 21 nm.

The optical properties of synthesized copper oxide nanoparticles were determined by Varian Cary 500 and Shimadzu UV 3600, shown in Figure 2. Using absorbance data, band gap and electronic transition type were also determined. UV absorption of synthesized nanoparticles was taken in ethanol solution followed by ultrasonic vibrations to get a transparent liquid. UV spectrum shows a distinct absorption peak around 208 nm, which agrees with the previously reported data [27]. The band gap and electronic transition type of synthesized nanoparticles were calculated using equation 2.

$$(ah\nu)^\gamma = A(h\nu - E_g) \dots \dots \dots (2)$$

where a is the absorption coefficient, h is Planck's constant, ν is the photon's frequency, A is the proportionality constant, E_g is the band gap energy, and γ denotes the nature of electronic transition ($\gamma = 2$ for direct allowed transition and $\gamma = 1/2$ for indirect allowed transitions). By extrapolating the linear part of the plot $(ah\nu)^{1/2}$ against $(h\nu)$, the band gap is determined to be 2.90 eV. A wider band gap than bulk CuO (1.85 eV) is due to a decrease in particle size [28].

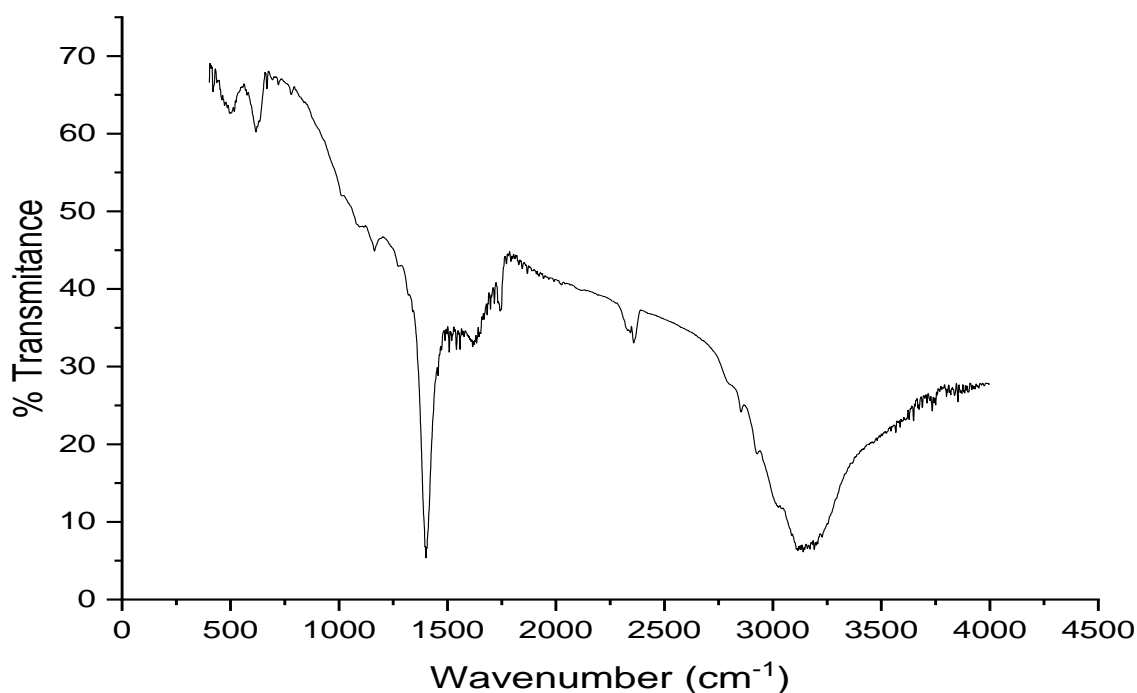


Figure 3. FTIR-spectrum of synthesized copper oxide nanoparticles.

Chemical composition and surface functionalization were done through Perkin Elmer, G-FTIR and FTIR spectrum was recorded in the range of 400-4000 cm^{-1} , as shown in Figure 3. The strong absorption band located at 3200-3450 cm^{-1} is due to the presence of milk, which is attributed to the hydroxyl group and H-bonded OH stretching vibrations; 1660 cm^{-1} is due to the disordered protein structure, which was attributed to a high content of proline residues, peaks around 1600-1700 cm^{-1} is due to the carbonyl stretching amide [21]. It has already been reported that secondary amines present in milk act as capping agents and stabilize nanoparticles. The peak at 1639 cm^{-1} represents the stretching vibration of the Cu-O bond of

copper(II) oxide nanoparticles [29]. Three peaks in the range of 450-650 cm^{-1} represent Cu-O stretching or CuO nanoparticle formation [30]. Among three peaks, a peak at 497 cm^{-1} was attributed to Cu-O stretching vibration along miller indices at 101 directions [31]. The FTIR spectra of the synthesized nanoparticles also show a peak at 617 cm^{-1} , which resembles the previously reported value [27]. The FTIR data confirms the molecular formula of synthesized nanoparticles as CuO.

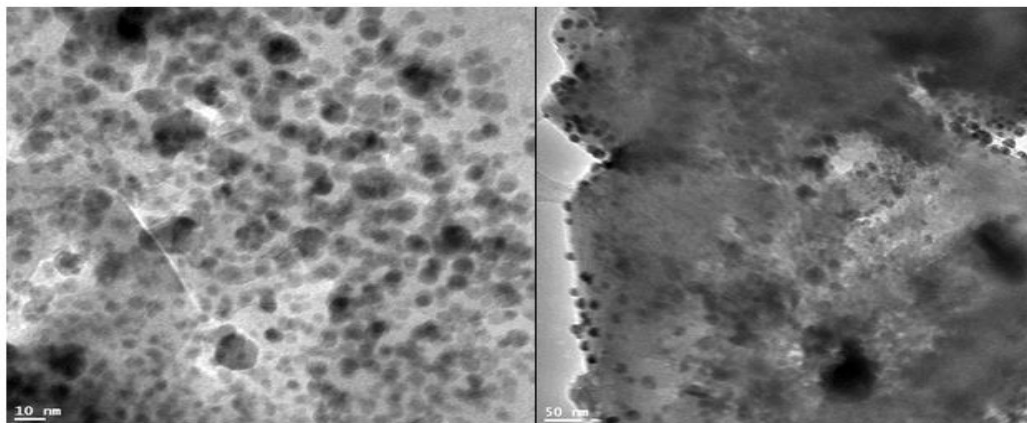


Figure 4. TEM images of synthesized copper oxide nanoparticles.

The size of synthesized nanoparticles was determined using Transmission Electron Microscope (TEM) JEOL, JEM 2100. TEM images of synthesized copper oxide nanoparticles are shown in Figure 4. The size of particles was determined by analyzing the TEM image with image J [32], which lies within the range of 16-26 nm, and the average size of synthesized nanoparticles is 23 nm, which is in good agreement with the XRD results. TEM images show some agglomeration among the crystalline shapes of copper oxide nanoparticles.

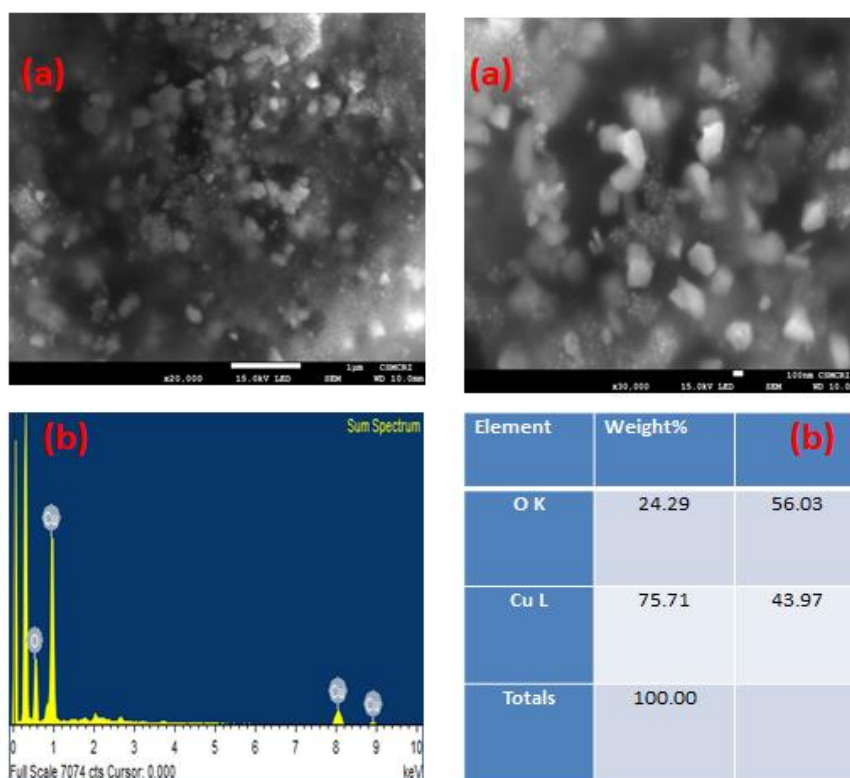


Figure 5. (a) SEM images of synthesized copper oxide nanoparticles; (b) EDX spectra of synthesized copper oxide nanoparticles.

The surface morphology and elemental composition of synthesized copper oxide nanoparticles were analyzed using SEM-EDX JEOL JSM 7100F, shown in Figure 5 (a, b). The SEM images confirm that the synthesized nanoparticles are cubical. The EDX spectrum of synthesized nanoparticles revealed copper peaks at 1 KeV and 8 KeV and the weight percent composition of copper and oxygen is 75.71% and 24.29%, respectively, representing the crystal's purity [33].

3.2. Antimicrobial potential.

The antimicrobial activity of synthesized copper oxide nanoparticles was analyzed against bacterial strains (*Bacillus subtilis*, *B. megaterium*, *Escherichia coli*, and *Serratia marcescens*) and fungal pathogens (*Fusarium solani*, *Paecilomyces variotii*, *Trametes hirsuta* and *Pythium afertile*). A nano-extract was prepared by dissolving 19 mg of synthesized copper oxide nanoparticles in 1 mL of ethanol to examine antimicrobial potential. The antibacterial and antifungal potential of nanoparticles were determined by the disc diffusion method and dual culture method, respectively.

3.2.1. Disc diffusion method.

For disc diffusion assay, the bacterial lawn was prepared using an overnight grown culture of each bacterial suspension (100 μ l) and inoculated over the agar, followed by uniformly spread with the help of a sterilized glass spreader. After that, 5 mm autoclaved filter paper (Whatman No. 1) discs carrying 30 μ L nano-extract (19 mg/mL in ethanol) were placed on respective plates. The plates were incubated at 25°C for 24 hours, and observations were recorded based on the zone of inhibition measurement around the disc.

3.2.2. Dual culture method.

For the dual culture method, two agar discs (5 mm in diameter) of a 7-day-old culture of the pathogen (was cut by sterile cork borer) and biocontrol agents were used. The pathogen agar disc was placed 1 cm away from the periphery of PDA Petri dish, while the agar disc of biocontrol agents was placed 1 cm away from the edge of the same petri plate on the opposite side of the pathogen. As a control, a same-size agar disc of 7-day-old culture of the pathogen was placed 1 cm away from the periphery of the Petri dish containing PDA. All plates were incubated at 27°C for 7 days. After incubation, the antagonistic activity was checked by measuring the growth radius of the pathogen in the dual plate (R2) and the growth radius of pathogencolony in the control plate (R1).

The disc diffusion and dual culture plate showing inhibitory potential against bacterial and fungal strains are presented in Figure 6. Among the tested bacterial strains, the nano-extract showed antibacterial activity against only *E. coli* (Table 1). However, the nano-extract showed inhibition potential against fungal pathogens, namely *Trametes hirsuta*, *Fusarium solani* (Table 1).

Table 1. Antibacterial and antifungal potential of copper oxide nanoparticles.

| Bacterial pathogen | ZOI (mm) |
|---------------------------|-----------------------|
| <i>E. coli</i> | 16 \pm 0.6 |
| Fungal pathogen | Inhibition (%) |
| <i>Trametes hirsuta</i> | 37 |
| <i>Fusarium solani</i> | 29 |

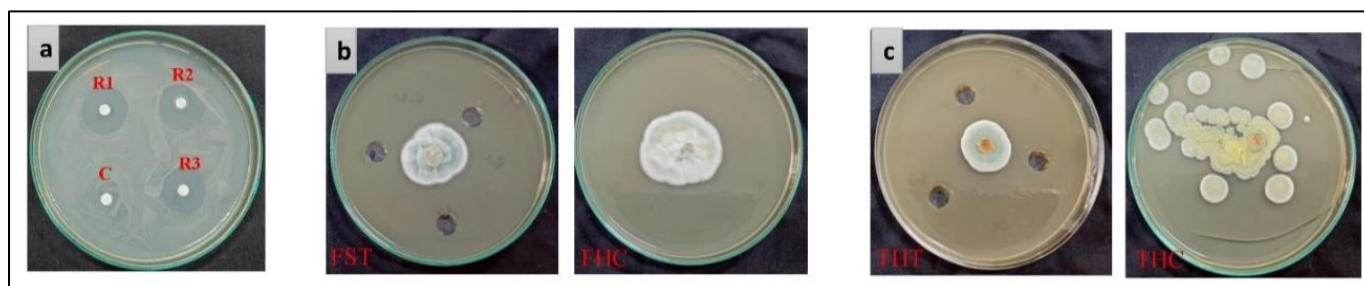


Figure 6. Antimicrobial activity of nanoparticles: (a) antibacterial (*E. coli*); (b) antifungal (*Fusarium solani*); (c) *Trametes hirsute*.

4. Conclusions

In the present study, the average sizes of synthesized copper oxide nanoparticles, which are crystalline, were found to be nearly 23 nm. The band gap was found to be 2.90 eV using Tauc's plot. The SEM-EDX result confirms that the synthesized nanoparticles are cubic, and the weight% of "Cu" and "O" were found to be 75.71% and 24.29%, respectively. The FTIR data confirms the copper oxide nanoparticles were found in the form of CuO. Synthesized nanoparticles showed antibacterial activity against *E. coli* and inhibition potential against fungal pathogens, namely *Trametes hirsuta* and *Fusarium solani*. This method is a preliminary step towards the new polyol method for nanoparticle synthesis due to the addition of milk. The biogenic approach using cow milk to synthesize copper oxide nanoparticles is a safe method, so these particles may have potential applications in pharmaceutical and medical sciences.

Funding

This research received no external funding.

Acknowledgments

The author wishes to thank UGC, New Delhi, for financial support. The authors are thankful to Prof. Raj N. Mehrotra, former President and Head of the Chemistry Department at Jodhpur University, for useful help with valuable suggestions.

Conflicts of Interest

The authors declare no conflict of interest.

References

1. Tortella, G. R.; Pieretti, J. C.; Rubilar, O.; Baldo, M.F.; Mendoza, A.B.; Diez, M. C.; Seabra, A. B. Silver, Copper and Copper Oxide Nanoparticles in the Fight against Human Viruses: Progress and Perspectives. *Critical Reviews in Biotechnology* **2021**, *42*, 431–449. <https://doi.org/10.1080/07388551.2021.1939260>.
2. Khatamifar, M.; Fatemi, S. J. Green Synthesis of Pure Copper Oxide Nanoparticles Using Quercus Infectoria Galls Extract, Thermal Behavior and Their Antimicrobial Effects. *Particulate Science and Technology* **2021**, *40*, 1–9. <https://doi.org/10.1080/02726351.2021.1901810>.
3. Patil, V. B.; Malode, S. J.; Mangasuli, S. N.; Tuwar, S. M.; Mondal, K.; Shetti, N. P. An Electrochemical Electrode to Detect Theophylline Based on Copper Oxide Nanoparticles Compositd with Graphene Oxide. *Micromachines* **2022**, *13*, 1166. <https://doi.org/10.3390/mi13081166>.
4. Shkir, M. Green Method for Synthesis and Characterization of Copper Oxide Nanoparticles Using Mulberry Plant Extract and Their Antibacterial, Antioxidant and Photocatalytic Activity. *Physica Scripta* **2022**, *97*, 105001. <https://doi.org/10.1088/1402-4896/ac8a7a>.

5. Siddiqui, H.; Qureshi, M. S.; Haque, F. Z. Effect of Copper Precursor Salts: Facile and Sustainable Synthesis of Controlled Shaped Copper Oxide Nanoparticles. *Optik* **2016**, *127*, 4726–4730. <https://doi.org/10.1016/j.ijleo.2016.01.118>.
6. Li, Y.; Lu, Y. L.; Wu, K.; Zhang, D.; Debliquy, M.; Zhang, C. Microwave-Assisted Hydrothermal Synthesis of Copper Oxide-Based Gas-Sensitive Nanostructures. *Rare Metals* **2021**, *40*, 1477–1493. <https://doi.org/10.1007/s12598-020-01557-4>.
7. Indhira, D.; Krishnamoorthy, M.; Ameen, F.; Bhat, S. A.; Arumugam, K.; Ramalingam, S.; Priyan, S. R.; Kumar, G. S. Biomimetic Facile Synthesis of Zinc Oxide and Copper Oxide Nanoparticles from *Elaeagnus Indica* for Enhanced Photocatalytic Activity. *Environmental Research* **2022**, *212*, 113323. <https://doi.org/10.1016/j.envres.2022.113323>.
8. Zhao, Y.; Zhu, J. J.; Hong, J. M.; Bian, N.; Chen, H. Y. Microwave-Induced Polyol-Process Synthesis of Copper and Copper Oxide Nanocrystals with Controllable Morphology. *European Journal of Inorganic Chemistry* **2004**, *2004*, 4072–4080. <https://doi.org/10.1002/ejic.200400258>.
9. Chan, Y.; Selvanathan, V.; Tey, L. H.; Akhtaruzzaman, Md.; Anur, F.; Djearamane, S.; Watanabe, A.; Aminuzzaman, M. Effect of Calcination Temperature on Structural, Morphological and Optical Properties of Copper Oxide Nanostructures Derived from *Garcinia Mangostana* L. Leaf Extract. *Nanomaterials* **2022**, *12*, 3589. <https://doi.org/10.3390/nano12203589>.
10. Esmail, E. R. T.; Golshan, M.; Kalajahi, M. S.; Mamaqani, H. R. Synthesis of Copper and Copper Oxide Nanoparticles with Different Morphologies Using Aniline as Reducing Agent. *Solid State Communications* **2021**, *334-335*, 1-9. <https://doi.org/10.1016/j.ssc.2021.114364>.
11. Guzman, M.; Arcos, M.; Dille, J.; Rousse, C.; Godet, S.; Malet, L. Effect of the Concentration and the Type of Dispersant on the Synthesis of Copper Oxide Nanoparticles and Their Potential Antimicrobial Applications. *ACS Omega* **2021**, *6*, 18576–18590. <https://doi.org/10.1021/acsomega.1c00818>.
12. Anand, G. T.; Sundaram, S. J.; Kanimozhi, K.; Nithiyavathi, R.; Kaviyarasu, K. Microwave Assisted Green Synthesis of CuO Nanoparticles for Environmental Applications. *Materials Today: Proceedings* **2021**, *36*, 427–434. <https://doi.org/10.1016/j.matpr.2020.04.881>.
13. Abdalamin, R. Q.; Khodair, Z. T.; Abd, A. N. Preparation and Characterization of Structural Properties for TiO₂ and CuO Nanostructures by Sol-Gel Technique. *Materials Today: Proceedings* **2022**, *57*, 539–544. <https://doi.org/10.1016/j.matpr.2022.01.417>.
14. Thangamani, J. G.; Pasha, S. K. K. Hydrothermal Synthesis of Copper (II) Oxide-Nanoparticles with Highly Enhanced BTEX Gas Sensing Performance Using Chemiresistive Sensor. *Chemosphere* **2021**, *277*, 1-13. <https://doi.org/10.1016/j.chemosphere.2021.130237>.
15. Hachem, K.; Ansari, M. J.; Saleh, R. O.; Kzar, H. H.; Al-Gazally, M. E.; Altimari, U. S.; Hussein, S. A.; Mohammed, H. T.; Hammid, A. T.; Kianfar, E. Methods of Chemical Synthesis in the Synthesis of Nanomaterial and Nanoparticles by the Chemical Deposition Method: A Review. *BioNanoScience* **2022**, *12*, 1032–1057. <https://doi.org/10.1007/s12668-022-00996-w>.
16. Grigore, M.; Biscu, E.; Holban, A.; Gestal, M.; Grumezescu, A. Methods of Synthesis, Properties and Biomedical Applications of CuO Nanoparticles. *Pharmaceuticals* **2016**, *9*, 1-14. <https://doi.org/10.3390/ph9040075>.
17. Sung, S. Y.; Kim, S. Y.; Jo, K. M.; Lee, J. H.; Kim, J. J.; Kim, S. H.; Chai, K.; Pearton, S. J.; Norton, D. P.; Heo, Y. W. Fabrication of P-Channel Thin-Film Transistors Using CuO Active Layers Deposited at Low Temperature. *Applied Physics Letters* **2010**, *97*, 222109–222109. <https://doi.org/10.1063/1.3521310>.
18. Zayyoun, B.; Bahmad, L.; Laânab, L.; Jaber, B. The Effect of pH on the Synthesis of Stable Cu₂O/CuO Nanoparticles by Sol-Gel Method in a Glycolic Medium. *Applied Physics A* **2016**, *122*, 1-6. <https://doi.org/10.1007/s00339-016-0024-9>.
19. Dahonog, L. A.; Vega, M.S.D.D.; Balela, M.D.L. pH-Dependent Synthesis of Copper Oxide Phases by Polyol Method. *Journal of Physics: Conference Series* **2019**, *1191*, 1-6. <https://doi.org/10.1088/1742-6596/1191/1/012043>.
20. Dawoud, T. M. S.; Pavitra, V.; Ahmad, P.; Syed, A.; Nagaraju, G. Photocatalytic Degradation of an Organic Dye Using Ag Doped ZrO₂ Nanoparticles: Milk Powder Facilitated Eco-Friendly Synthesis. *Journal of King Saud University - Science* **2020**, *32*, 1872–1878. <https://doi.org/10.1016/j.jksus.2020.01.040>.
21. Pandey, S.; Klerk, C. D.; Kim, J.; Kang, M.; Kankeu, E. F. Eco Friendly Approach for Synthesis, Characterization and Biological Activities of Milk Protein Stabilized Silver Nanoparticles. *Polymers* **2020**, *12*, 1-18. <https://doi.org/10.3390/polym12061418>.

22. Sahil, S. T.; Promi, A. T.; Hossain, Md. K.; Ahmad, N.; Al Muhit, Md. A.; Dey, S. C.; Ashaduzzaman, Md. Cow Milk Lactose Inspired Fabrication of Zinc Oxide (ZnO) Nanorods for Bio-Applications. *Inorganic and Nano-Metal Chemistry* **2022**, 1–9. <https://doi.org/10.1080/24701556.2022.2034006>.
23. Yao, W.; Yu, S. H.; Zhou, Y.; Jiang, J.; Wu, Q. S.; Zhang, L.; Jiang, J. Formation of Uniform CuO Nanorods by Spontaneous Aggregation: Selective Synthesis of CuO, Cu₂O, and Cu Nanoparticles by a Solid–Liquid Phase Arc Discharge Process. *Journal of Physical Chemistry B* **2005**, *109*, 14011–14016. <https://doi.org/10.1021/jp0517605>.
24. Habibi, M. H.; Karimi, B. Effect of the Annealing Temperature on Crystalline Phase of Copper Oxide Nanoparticle by Copper Acetate Precursor and Sol–Gel Method. *Journal of Thermal Analysis and Calorimetry* **2014**, *115*, 419–423. <https://doi.org/10.1007/s10973-013-3255-4>.
25. Ghidan, A. Y.; Al-Antary, T. M.; Awwad, A. M. Green Synthesis of Copper Oxide Nanoparticles Using Punica Granatum Peels Extract: Effect on Green Peach Aphid. *Environmental Nanotechnology, Monitoring & Management* **2016**, *6*, 95–98. <https://doi.org/10.1016/j.enmm.2016.08.002>.
26. Holzwarth, U.; Gibson, N. The Scherrer Equation versus the “Debye-Scherrer Equation.” *Nature Nanotechnology* **2011**, *6*, 534–534. <https://doi.org/10.1038/nnano.2011.145>.
27. Prasad, J.; Kumar, V.; Chandra, B.; Kandpal, N. D. Synthesis and Characterization of Copper Oxide Nanoparticles Using Different Precursor. *Rasayan Journal of Chemistry* **2022**, *15*, 72–81. <https://doi.org/10.31788/rjc.2022.1516579>.
28. Mohammadikish, M.; Akradi, A. A. Synthesis and Optical Band Gap Determination of CuO Nanoparticles from Salen-Based Infinite Coordination Polymer Nanospheres. *Materials Research Express* **2019**, *6*, 1–6. <https://doi.org/10.1088/2053-1591/aaf8e3>.
29. Raul, P. K.; Senapati, S.; Sahoo, A. K.; Umlong, I. M.; Devi, R. R.; Thakur, A. J.; Veer, V. CuO Nanorods: A Potential and Efficient Adsorbent in Water Purification. *RSC Adv.* **2014**, *4*, 40580–40587. <https://doi.org/10.1039/c4ra04619f>.
30. Swarnkar, R. K.; Singh, S. K.; Gopal R. Effect of Aging on Copper Nanoparticles Synthesized by Pulsed Laser Ablation in Water: Structural and Optical Characterizations. *Bulletin of Materials Science* **2011**, *34*, 1363–1369. <https://doi.org/10.1007/s12034-011-0329-4>.
31. Ethiraj, A. S.; Kang, D. J. Synthesis and Characterization of CuO Nanowires by a Simple Wet Chemical Method. *Nanoscale Research Letters* **2012**, *7*, 1–5. <https://doi.org/10.1186/1556-276x-7-70>.
32. Schneider, C. A.; Rasband, W. S.; Eliceiri, K. W. NIH Image to ImageJ: 25 Years of Image Analysis. *Nature Methods* **2012**, *9*, 671–675. <https://doi.org/10.1038/nmeth.2089>.
33. Khan, M. A.; Nayan, N.; Shadiullah, S.; Ahmad, M. K.; Soon, C. F. Surface Study of CuO Nanopetals by Advanced Nanocharacterization Techniques with Enhanced Optical and Catalytic Properties. *Nanomaterials* **2020**, *10*, 1–18. <https://doi.org/10.3390/nano10071298>.